arXiv:1606.05085v1 [math.NA] 16 Jun 2016

A priori error estimates and computational studies for a Fermi pencil-beam equation

M. Asadzadeh[*,1], L. Beilina[*], M. Naseer[**] and C. Standar[*]

Keywords: Fermi and Fokker-Planck pencil-beam equations, adaptive finite element method, duality argument, a priori error estimates, efficiency, reliability

Abstract

We derive a priori error estimates for the standard Galerkin and streamline diffusion finite element methods for the Fermi pencil-beam equation obtained from a fully three dimensional Fokker-Planck equation in space $\mathbf{x} = (x, y, z)$ and velocity $\tilde{\mathbf{v}} = (\mu, \eta, \xi)$ variables. The Fokker-Planck term appears as a Laplace-Beltrami operator in the unit sphere. The diffusion term in the Fermi equation is obtained as a projection of the FP operator onto the tangent plane to the unit sphere at the pole $(1, 0, 0)$ and in the direction of $\mathbf{v}_0 = (1, \eta, \xi)$. Hence the Fermi equation, stated in three dimensional spatial domain $\mathbf{x} = (x, y, z)$, depends only on two velocity variables $\mathbf{v} = (\eta, \xi)$. Since, for a certain number of cross-sections, there is a closed form analytic solution available for the Fermi equation, hence an a posteriori error estimate procedure is unnecessary and in our adaptive algorithm for local mesh refinements we employ the a priori approach. Different numerical examples, in two space dimensions are justifying the theoretical results. Implementations show significant reduction of the computational error by using our adaptive algorithm.

1 Introduction

This work is a further development of studies in [2]-[5] where adaptive finite element method was proposed for a reduction of computational cost in numerical approximation for pencil-beam equations. However, focusing in theoretical convergence and stability aspects, except some special cases with limited amount of implementation in [3] and [5], the detailed numerical tests were postponed to future works. Here, first we construct and analyze fully discrete schemes using both standard Galerkin and flux correcting streamline diffusion finite element methods for the Fermi pencil beam equation in three dimensions. We consider the direction of x-axis as the penetration direction of the beam particles, in the two-dimensional

[*,1] Corresponding author, [*] Department of Mathematical Sciences, Chalmers University of Technology and Gothenburg University, SE-42196 Gothenburg, Sweden, e-mail: mohammad@chalmers.se, larisa@chalmers.se, standarc@chalmers.se, [**] e-mail: na.seer@hotmail.com

transverse spatial domain $\Omega_\perp := \{x_\perp | x_\perp := (y,z)\}$, moving with velocities in $\Omega_{\mathbf{v}} : \{(\eta,\xi)\}$, (where we have assumed $\mu \equiv 1$). We have derived our error estimates, in this geometry, while in numerical implementations we have also considered examples in lower dimensions.

More specifically, our study concerns a "pencil beam" of neutral or charged particles that are normally incident on a slab of finite thickness at the spatial origin $(0,0,0)$ and in the direction of the positive x-axis. The governing equation for the pencil beam problem is the Fermi equation which is obtained by two equivalent approaches (see [7]): either as an asymptotic limit of the linear Boltzmann equation as the transport cross-section $\sigma_{tr} \to 0$ and the total cross-section $\sigma_t \to \infty$, or as an asymptotic limit in Taylor expansion of angular flux with respect to the velocity where the terms with derivatives of order three or higher are ignored. This procedure rely on a approach that follows the Fokker-Planck development.

The Boltzmann transport equation modeling the energy independent pencil beam process can be written as a two-point boundary value problem viz,

$$\mu\frac{\partial u}{\partial x} + \eta\frac{\partial u}{\partial y} + \xi\frac{\partial u}{\partial z} = \int_{S^2} \sigma_s(\mathbf{v}\cdot\mathbf{v}')[u(\mathbf{x},\mathbf{v}') - u(\mathbf{x},\mathbf{v})]\, d^2\mathbf{v}', \quad 0 < x < 1, \tag{1.1}$$

where $\mathbf{x} = (x,y,z)$ and $\mathbf{v} = (\mu,\eta,\xi)$ are the space and velocity vectors, respectively. The model problem concerns sharply forward peaked beam of particles entering the spatial domain at $x = 0$:

$$u(0,y,z,\mathbf{v}) = \delta(y)\delta(z)\frac{\delta(1-\mu)}{2\pi}, \qquad 0 < \mu \leq 1, \tag{1.2}$$

which are demising leaving the domain at $x = 1$ (or $x = L$), viz, e.g.

$$u(1,y,z,\mathbf{v}) = 0, \qquad -1 \leq \mu < 0. \tag{1.3}$$

In the realm of the Boltzmann transport equation (1.1) an overview of the transport theory of charged particles can be found in [13]. In this setting a few first coefficients in a Legendre polynomial expansion for σ_s and its integral σ_t are parameters corresponding to some physical quantities of vital importance. For instance, the slab width in the unit of mean free path: σ_t^{-1}, is the reciprocal of the total cross-section

$$\sigma_t = 2\pi\int_{-1}^{1}\sigma_s(\omega)\, d\omega.$$

In the absorptionless case, the differential scattering cross section is given by

$$\sigma_s(\omega) = \sigma_t\sum_{k=0}^{\infty}\frac{2k+1}{4\pi}c_k P_k(\omega), \quad c_0 = 1, \quad c_1 = \omega, \tag{1.4}$$

with $P_k(\omega)$ being the Legendre polynomial of degree k. The Fokker-Planck approximation to problem (1.1), is based on using spherical harmonics expansions and yields the following, degenerate type partial differential equation

$$\mu\frac{\partial u}{\partial x} + \eta\frac{\partial u}{\partial y} + \xi\frac{\partial u}{\partial z} = \frac{\sigma_{tr}}{2}\Delta_{\mathbf{V}}u(\mathbf{x},\mathbf{v}), \qquad 0 < x < 1, \tag{1.5}$$

associated with the same boundary data as (1.2) and (1.3), and with $\Delta_{\mathbf{V}}$ denoting the Laplace-Beltrami operator

$$\Delta_{\mathbf{V}} := \Big[\frac{\partial}{\partial\mu}(1-\mu^2)\frac{\partial}{\partial\mu} + \frac{1}{1-\mu^2}\frac{\partial^2}{\partial\phi^2}\Big]. \tag{1.6}$$

Here, ϕ is the angular variable appearing in the polar representation $\eta = \sqrt{1-\mu^2}\cos\phi$, $\xi = \sqrt{1-\mu^2}\sin\phi$. Further, σ_{tr} is the transport cross-section defined by

$$\sigma_{tr} = \sigma_t(1-\omega).$$

A thorough exposition of the Fokker-Planck operator as an asymptotic limit is given by Pomraning in [14]. Due to successive asymptotic limits used in deriving the Fokker-Planck approximation, it is not obvious that this approximation is sufficiently accurate to be considered as a model for the pencil beams. However, for sufficiently small transport cross-section $\sigma_{tr} << 1$, Fermi proposed the following form of, projected, Fokker-Planck model:

$$\frac{\partial u}{\partial x} + \eta\frac{\partial u}{\partial y} + \xi\frac{\partial u}{\partial z} = \frac{\sigma_{tr}}{2}\Big(\frac{\partial^2}{\partial\eta^2} + \frac{\partial^2}{\partial\xi^2}\Big)u(\mathbf{x},\mathbf{v}), \qquad 0 < x < 1, \tag{1.7}$$

with

$$u(0,y,z,\eta,\xi) = \delta(y)\delta(z)\delta(\eta)\delta(\xi). \tag{1.8}$$

Fermi's approach is different from the asymptotic ones and uses physical reasoning based on modeling cosmic rays. Note that the Fokker-Planck operator on the right hand side of (1.5), i.e. (1.6), is the Laplacian on the unit sphere. The tangent plane to the unit sphere S^2 at the point $\mu_0 := (1,0,0)$ is an $\mathcal{O}(\eta^2+\xi^2)$ approximation to the S^2 at the vicinity of μ_0. Extending (η,ξ) to $\mathbb{R}^2$, the Fourier transformation with respect to y, z, η, and ξ, assuming constant σ_{tr}, yields the following exact solution for the angular flux

$$u(x,y,z,\eta,\xi) = \frac{3}{\pi^2\sigma_{tr}^2x^4}\exp\Big[-\frac{2}{\sigma_{tr}}\Big(\frac{\eta^2+\xi^2}{x} - 3\frac{y\eta+z\xi}{x^2} + 3\frac{y^2+z^2}{x^3}\Big)\Big]. \tag{1.9}$$

The closed form solution (1.9) was first derived by Fermi as referred in [16]. Eyges [10] has extended this exact solution to the case of an x-depending $\sigma_{tr} = \sigma_{tr}(x)$. However, for the general case of $\sigma_{tr}(\mathbf{x}) = \sigma_{tr}(x,y,z)$, the closed-form analytic solution is not known. To obtain the scalar flux we integrate (1.9) over $(\eta,\xi) \in \mathbb{R}^2$:

$$\widetilde{U}(x,y,z) = \int_{\mathbb{R}^2} u(x,y,z,\eta,\xi)\,d\eta d\xi = \frac{3}{2\pi\sigma_{tr}x^3}\exp\Big[-\frac{3}{2\sigma_{tr}}\Big(\frac{y^2+z^2}{x^3}\Big)\Big]. \tag{1.10}$$

Equation (1.10) satisfies the transverse diffusion equation

$$\frac{\partial\widetilde{U}}{\partial x} = \frac{\sigma_{tr}x^2}{2}\Big(\frac{\partial^2\widetilde{U}}{\partial y^2} + \frac{\partial^2\widetilde{U}}{\partial z^2}\Big), \tag{1.11}$$

with

$$\widetilde{U}(0,y,z) = \delta(y)\delta(z). \tag{1.12}$$

Restricted to bounded phase-space domain, Fermi equation (1.7) can be written as the following "initial" boundary value problem

$$\begin{cases} u_x + \mathbf{v}\cdot\nabla_\perp u = \frac{\sigma_{tr}}{2}\Delta_{\mathbf{V}} u & \text{in} \quad \Omega := \Omega_{\mathbf{x}} \times \Omega_{\mathbf{v}}, \\ \nabla_{\mathbf{v}} u(x, x_\perp, \mathbf{v}) = 0 & \text{for} \quad (x, x_\perp, \mathbf{v}) \in \Omega_{\mathbf{x}} \times \partial\Omega_{\mathbf{v}}, \\ u(0, x_\perp, \mathbf{v}) = u_0(x_\perp, \mathbf{v}) & \text{for} \quad (x_\perp, \mathbf{v}) \in \Omega_{x_\perp} \times \Omega_{\mathbf{v}} =: \Omega_\perp, \\ u(x, x_\perp, \mathbf{v}) = 0 & \text{on} \quad \Gamma^-_{\tilde\beta} \setminus \{(0, x_\perp, \mathbf{v})\}, \end{cases} \tag{1.13}$$

where $\mathbf{v} = (\eta, \xi)$, $\nabla_\perp = (\partial/\partial y, \partial/\partial z)$ and

$$\Gamma^-_{\tilde\beta} := \{(x, x_\perp, \mathbf{v}) \in \partial\Omega, \mathbf{n}\cdot\tilde\beta < 0\} \tag{1.14}$$

is the inflow boundary with respect to the characteristic line $\tilde\beta := (1, \mathbf{v}, 0, 0)$ and $\mathbf{n}$ is the outward unit normal to the boundary $\partial\Omega$. Note that, to derive energy estimates, the associated boundary data (viewed as a replacement for the initial data) at $x = 0$ is, in a sense, approximating the product of the Dirac's delta functions on the right hand side of (1.8). Assuming that we can use separation of variables, we may write the data function u_0 as product of two functions $f(x_\perp)$ and $g(\mathbf{v})$,

$$u_0(x_\perp, \mathbf{v}) = f(x_\perp)g(\mathbf{v}).$$

The regularity of these functions have substantial impact in deriving theoretical stabilities and are essential in robustness of implemented results.

2 The phase-space standard Galerkin procedure

Below we introduce a framework that concerns a standard Galerkin discretization based on a quasi-uniform triangulation of the phase-space domain $\Omega_\perp := \Omega_{x_\perp} \times \Omega_{\mathbf{v}} := I_\perp \times \Omega_{\mathbf{v}}$, where $I_\perp := I_y \times I_z$. This is an extension of our studies in two-dimensions in a flatland model [3]. Previous numerical approaches are mostly devoted to the study of the one-dimensional problem see, e.g. [12] and [15].

Here we consider triangulations of the rectangular domains $I_\perp$ and $\Omega_{\mathbf{v}} := I_\eta \times I_\xi$ into triangles $\tau_\perp$ and $\tau_{\mathbf{v}}$, and with the corresponding mesh parameters $h_\perp$ and $h_{\mathbf{v}}$, respectively. Then a general polynomial approximation of degree $\leq r$ can be formulated in $\mathbb{P}_r(\tau) := \mathbb{P}_r(\tau_\perp) \otimes \mathbb{P}_r(\tau_{\mathbf{v}})$. These polynomial spaces are more specified in the implementation section. We will assume a minimal angle condition on the triangles $\tau_\perp$ and $\tau_{\mathbf{v}}$ (see e.g. [8]). Treating the beams entering direction x similar to a time variable, we let $\mathbf{n} := \mathbf{n}(y, z, \mathbf{v})$ be the outward unit normal to the boundary of the phase-space domain $\Omega_{x_\perp} \times \Omega_{\mathbf{v}}$ at $(y, z, \mathbf{v}) \in \partial\Omega_\perp$ where $\partial\Omega_\perp := (\partial\Omega_{x_\perp} \times \Omega_{\mathbf{v}}) \cup (\Omega_{x_\perp} \times \partial\Omega_{\mathbf{v}})$. Now set $\beta := (\mathbf{v}, 0, 0)$ and define the inflow (outflow) boundary as

$$\Gamma_\beta^{-(+)} := \{(x_\perp, \mathbf{v}) \in \Gamma := \partial\Omega_\perp : \mathbf{n} \cdot \beta < 0\,(> 0)\}. \tag{2.1}$$

We shall also need an abstract finite element space as a subspace of a function space of Sobolev type, viz:

$$\mathcal{V}_{h,\beta} \subset H^1_\beta := \{w \in H^1(I_\perp \times \Omega_\mathbf{v}) : w = 0 \text{ on } \Gamma^-_\beta\}. \tag{2.2}$$

Now for all $w \in H^1(I_\perp \times \Omega_\mathbf{v}) \cap H^r(I_\perp \times \Omega_\mathbf{v})$ a classical standard estimate reads as

$$\inf_{\chi \in \mathcal{V}_{h,\beta}} ||w - \chi||_j \leq C h^{\alpha - j} ||w||_\alpha, \quad j = 1, 2, \quad 1 \leq \alpha \leq r \quad \text{and } h = \max(h_\perp, h_\mathbf{v}). \tag{2.3}$$

To proceed let $\tilde{u}$ be an auxiliary interpolant of the solution u for the equation (1.13) defined by

$$\mathcal{A}(u - \tilde{u}, \chi)_\perp = 0, \quad \forall\, \chi \in \mathcal{V}_{h,\beta}, \tag{2.4}$$

where

$$\mathcal{A}(u, w)_\perp = (u_x, w)_{\Omega_\perp} + (\mathbf{v} \cdot \nabla_\perp u, w)_{\Omega_\perp}, \tag{2.5}$$

and $(\cdot,\cdot)_\perp := (\cdot,\cdot)_{\Omega_\perp} = (\cdot,\cdot)_{I_\perp \times \Omega_\mathbf{v}}$.

With these notation the weak formulation for the problem (1.13) can be written as follows: for each $x \in (0, L]$, find $u(x,\cdot) \in H^1_\beta$ such that,

$$\begin{cases} \mathcal{A}(u, \chi)_\perp + \frac{1}{2}(\sigma_{tr} \nabla_\mathbf{v} u, \nabla_\mathbf{v} \chi)_\perp = 0 & \forall \chi \in H^1_\beta, \\ u(0, x_\perp, \mathbf{v}) = u_0(x_\perp, \mathbf{v}) & \text{for } (x_\perp, \mathbf{v}) \in \Gamma^+_\beta, \\ u(x, x_\perp, \mathbf{v}) = 0 & \text{on } \Gamma^-_\beta \setminus \{(0, x_\perp, \mathbf{v})\}. \end{cases} \tag{2.6}$$

Our objective is to solve the following finite element approximation for the problem (2.6): for each $x \in (0, L]$, find $u_h(x,\cdot) \in \mathcal{V}_{h,\beta}$ such that,

$$\begin{cases} \mathcal{A}(u_h, \chi)_\perp + \frac{1}{2}(\sigma_{tr} \nabla_\mathbf{v} u_h, \nabla_\mathbf{v} \chi)_\perp = 0 & \forall \chi \in \mathcal{V}_{h,\beta}, \\ u_h(0, x_\perp, \mathbf{v}) = u_{0,h}(x_\perp, \mathbf{v}) & \text{for } (x_\perp, \mathbf{v}) \in \Gamma^+_\beta, \\ u_h(x, x_\perp, \mathbf{v}) = 0 & \text{on } \Gamma^-_\beta \setminus \{(0, x_\perp, \mathbf{v})\}, \end{cases} \tag{2.7}$$

where $u_{0,h}(x_\perp, \mathbf{v}) = \tilde{u}(0, x_\perp, \mathbf{v})$.

2.1 A fully discrete scheme

For a partition of the interval $[0, L]$ into the subintervals $I_m := (x_{m-1}, x_m), m = 1, 2, \ldots, M$ with $k_m := |I_m| := x_m - x_{m-1}$, a finite element approximation U with continuous linear functions $\psi_m(x)$ on I_m can be written as:

$$u_h(x, x_\perp, \mathbf{v}) = U_{m-1}(x_\perp, \mathbf{v})\psi_{m-1}(x) + U_m(x_\perp, \mathbf{v})\psi_m(x), \tag{2.8}$$

where $x_\perp := (y, z)$ and

$$\psi_{m-1}(x) = \frac{x_m - x}{k_m}, \qquad \psi_m(x) = \frac{x - x_{m-1}}{k_m}. \tag{2.9}$$

Hence, the setting (2.8)-(2.9) may be considered for an iterative, e.g. backward Euler, scheme with continuous piecewise linear or discontinuous (with jump discontinuities at grid points x_m) piecewise linear functions for whole $I_x = [0, L]$.

To proceed we consider a normalized, rectangular domain $\Omega_{\mathbf{V}}$ for the velocity variable $\mathbf{v}$, as $(\eta, \xi) \in [-1, 1] \times [-1, 1]$ and assume a uniform, "central adaptive" discretization mesh viz:

$$\Omega_{\mathbf{v}}^N := \left\{ \mathbf{v}_{i,j} \subset \Omega_{\mathbf{v}} \middle| \mathbf{v}_{i,j} = (\eta_i, \xi_j) := \left(\sin \frac{i\pi}{2n}, \sin \frac{j\pi}{2n} \right),\ i, j = 0, \pm 1, \dots \pm n \right\}, \tag{2.10}$$

where $N = (2n+1)^2$. Further we assume that U has compact support in $\Omega_{\mathbf{V}}$. By a standard approach one can show that, for each $m = 1, 2, \dots, M$, a finite element or finite difference solution U_m^N obtained using the discretization (2.10) of the velocity domain $\Omega_{\mathbf{v}}$, satisfies the $L_2(\Omega_{\mathbf{v}})$ error estimate

$$||U_m - U_m^N||_{L_2(\Omega_{\mathbf{v}})} \leq \frac{C}{N^2} ||D_{\mathbf{V}}^2 U_m(x_\perp, \cdot)||_{L_2(\Omega_{\mathbf{v}})}. \tag{2.11}$$

Now we introduce a final, finite element, discretization using continuous piecewise linear basis functions $\varphi_j(x_\perp)$, on a partition $\mathcal{T}_h$ of the spatial domain $\Omega_{x_\perp}$, on a quasi-uniform triangulation with the mesh parameter h and obtain the fully discrete solution $U_m^{N,h}$. We introduce discontinuities on the direction of entering beam (on the x-direction). We also introduce jumps appearing in passing a collision site; say x_m, as the difference between the values at x_m^- and x_m^+:

$$\Big[U_m\Big] := U_m^+ - U_m^-, \qquad U_m^\pm := \lim_{s \to 0} U(x_m \pm s, x_\perp, \mathbf{v}). \tag{2.12}$$

Due to the hyperbolic nature of the problem in $x_\perp$, for the solutions in the Sobolev space $H^{k+1}(\cdot, x_\perp, \mathbf{v})$, (see Adams [1] for the exact definitions of the Sobolev norms and spaces) the final finite element approximation yields an $L_2(\Omega_{x_\perp})$ error estimate viz,

$$||U_m^N - U_m^{N,k}||_{L_2(\Omega_{x_\perp})} \leq C h^{k+1/2} ||U_m^N(x_\perp, \cdot)||_{H^{k+1}(\Omega_{x_\perp})}. \tag{2.13}$$

To be specific, for each m and each $\mathbf{v}_{i,j} \in \Omega_{\mathbf{v}}$ we obtain a spatially continuous version of the equations system (1.13) where, for u, we insert

$$U_m(x_\perp, \mathbf{v}_{i,j}) = \sum_{k=1}^{K} U_{m,k}(\mathbf{v}_{i,j}) \varphi_k(x_\perp). \tag{2.14}$$

Thus for each $\mathbf{v}_{i,j} \in \Omega_{\mathbf{v}}$ a variational formulation for a *space-time like* discretization in $(x, x_\perp)$ of (2.8) reads as follows: find $U \in \mathcal{V}_{h,\beta}$ such that

$$\begin{aligned} \int_{I_m} \int_{\Omega_{x_\perp}} U_x(x, x_\perp, \mathbf{v}_{i,j}) \varphi_k(x_\perp) dx_\perp dx + \int_{I_m} \int_{\Omega_{x_\perp}} \mathbf{v}_{i,j} \cdot \nabla_\perp U(x, x_\perp, \mathbf{v}_{i,j}) \varphi_k(x_\perp) dx_\perp dx \\ = \int_{I_m} \int_{\Omega_{x_\perp}} \frac{\sigma_{tr}}{2} \Delta_{\mathbf{V}} U(x, x_\perp, \mathbf{v}_{i,j}) \varphi_k(x_\perp) dx_\perp dx, \qquad \forall\ \varphi_k \in \mathcal{V}_{h,\beta}, \end{aligned} \tag{2.15}$$

where

$$\mathcal{V}_{h,\beta} := \{w \in \mathcal{V}_\beta | w_{|\tau} \in \mathbb{P}_1(\tau), w \text{ is continuous}\}. \tag{2.16}$$

This yields

$$\begin{aligned}
&\int_{\Omega_{x_\perp}} \Big(U_m(x_\perp, \mathbf{V}_{i,j}) - U_{m-1}(x_\perp, \mathbf{v}_{i,j})\Big)\varphi_k(x_\perp)dx_\perp + \frac{k_m}{2}\int_{\Omega_{x_\perp}} \mathbf{v}_{i,j}\cdot\nabla_\perp U_m(x_\perp, \mathbf{V}_{i,j})\varphi_k(x_\perp)dx_\perp \\
&\quad + \frac{k_m}{2}\int_{\Omega_{x_\perp}} \mathbf{v}_{i,j}\cdot\nabla_\perp U_{m-1}(x_\perp, \mathbf{v}_{i,j})\varphi_k(x_\perp)dx_\perp \\
&\quad = \frac{\sigma_{tr}}{2}\frac{k_m}{2}\int_{\Omega_{x_\perp}} \Delta_{\mathbf{v}} U_m(x_\perp, \mathbf{v}_{i,j})\varphi_k(x_\perp)dx_\perp + \frac{\sigma_{tr}}{2}\frac{k_m}{2}\int_{\Omega_{x_\perp}} \Delta_{\mathbf{v}} U_{m-1}(x_\perp, \mathbf{v}_{i,j})\varphi_k(x_\perp)dx_\perp.
\end{aligned} \tag{2.17}$$

Such an equation would lead to a linear system of equations which in compact form can be written as the following matrix equation

$$\begin{aligned}
&MU_m(\mathbf{v}_{i,j}) - MU_{m-1}(\mathbf{v}_{i,j}) + \frac{k_m}{2}C_{\mathbf{v}_{i,j}}U_m(\mathbf{v}_{i,j}) + \frac{k_m}{2}C_{\mathbf{v}_{i,j}}U_{m-1}(\mathbf{v}_{i,j}) \\
&\qquad = \frac{\sigma_{tr}}{2}\frac{k_m}{2}\Delta_{\mathbf{v}}MU_m(\mathbf{v}_{i,j}) + \frac{\sigma_{tr}}{2}\frac{k_m}{2}\Delta_{\mathbf{v}}MU_{m-1}(\mathbf{v}_{i,j})
\end{aligned} \tag{2.18}$$

Now considering $\mathbf{v}$-continuous version of (2.18):

$$\begin{aligned}
&MU_m(\mathbf{v}) - MU_{m-1}(\mathbf{v}) + \frac{k_m}{2}C_{\mathbf{V}}U_m(\mathbf{v}) + \frac{k_m}{2}C_{\mathbf{V}}U_{m-1}(\mathbf{v}) \\
&\qquad = \frac{\sigma_{tr}}{2}\frac{k_m}{2}\Delta_{\mathbf{V}}MU_m(\mathbf{v}) + \frac{\sigma_{tr}}{2}\frac{k_m}{2}\Delta_{\mathbf{V}}MU_{m-1}(\mathbf{v}),
\end{aligned} \tag{2.19}$$

we may write

$$U_m(x_\perp, \mathbf{v}) = \sum_{k=1}^{K}\sum_{j=1}^{J} U_{m,k,j}\chi_j(\mathbf{v})\varphi_k(x_\perp). \tag{2.20}$$

Then a further variational form is obtained by multiplying (2.19) by χ_j, $j = 1, 2, \ldots, J$ and integrating over $\Omega_{\mathbf{V}}$:

$$\begin{aligned}
&\Big(M_{x_\perp}\otimes M_{\mathbf{v}}\Big)U_m + \frac{k_m}{2}\Big(C_{x_\perp}\otimes \widetilde{M}_{\mathbf{v}}\Big)U_m + \frac{\sigma_{tr}}{2}\frac{k_m}{2}\Big(S_{\mathbf{v}}\otimes M_{x_\perp}\Big)U_m \\
&\quad = \Big(M_{x_\perp}\otimes M_{\mathbf{v}}\Big)U_{m-1} - \frac{k_m}{2}\Big(C_{x_\perp}\otimes \widetilde{M}_{\mathbf{v}}\Big)U_{m-1} - \frac{\sigma_{tr}}{2}\frac{k_m}{2}\Big(S_{\mathbf{v}}\otimes M_{x_\perp}\Big)U_{m-1},
\end{aligned} \tag{2.21}$$

where $\otimes$ represents tensor products with the obvious notations for the coefficient matrices $M_{x_\perp}$, $M_{\mathbf{v}}$ being the mass-matrices in spatial and velocity variables, $C_{x_\perp}$ is the convection matrix in space, $\widetilde{M}_{\mathbf{v}} := \mathbf{v}\otimes M_{\mathbf{v}}$ corresponds to the spatial convection terms with the coefficient $\mathbf{v}$: $\mathbf{v}\cdot\nabla_\perp$, and finally $S_{\mathbf{v}}$ is the stiffness matrix in $\mathbf{v}$.

Now, given an initial beam configuration, $U_0 = u_0$, our objective is to use an iteration algorithm as the finite element version above or the corresponding equivalent backward Euler

(or Crank-Nicolson) approach for discretization in the $x_\perp$ variable, and obtain successive U_m-values at the subsequent discrete $x_\perp$-levels. To this end the delicate issues of an initial data viz (1.8), as a product of Dirac delta functions, as well as the desired dose to the target that imposes the model to be transferred to a case having an *inverse problem* nature are challenging practicalities.

2.1.1 Standard stability estimates

We use the notion of the scalar products over a domain $\mathbf{D}$ and its boundary $\partial\mathbf{D}$ as $(\cdot,\cdot)_{\mathbf{D}}$ and $\langle\cdot,\cdot\rangle_{\partial\mathbf{D}}$, respectively. Here, $\mathbf{D}$ can be $\Omega := I_x \times \Omega_{\mathbf{x}} \times \Omega_{\mathbf{v}}$, $I_x \times \Omega_{\mathbf{x}}$, $\Omega_{\mathbf{x}} \times \Omega_{\mathbf{v}}$, or possibly other relevant domains in the problem. Below we state and prove a stability lemma which, in some adequate norms, guarantees the control of the solution for the continuous problem by the data. The lemma is easily extended to the case of approximate solution.

We derive the stability estimate using the triple norm

$$|||w|||_\beta^2 = \int_0^L \int_{\Gamma_\beta^+} w^2(\mathbf{n}\cdot\beta)\, d\Gamma dx + ||\sigma_{tr}^{1/2}\nabla_{\mathbf{v}} w||_{L_2(\Omega)}^2. \tag{2.22}$$

Lemma 2.1. *For u satisfying* (1.13) *we have the stability estimates*

$$\sup_{x\in I_x} \|u(x,\cdot,\cdot)\|_{L_2(\Omega_\perp\times\Omega_{\mathbf{v}})} \le \|u_0(\cdot,\cdot)\|_{L_2(\Omega_\perp\times\Omega_{\mathbf{v}})}, \tag{2.23}$$

and

$$|||u|||_\beta \le \|u_0(\cdot,\cdot)\|_{L_2(\Omega_\perp\times\Omega_{\mathbf{v}})}. \tag{2.24}$$

Proof. We let $\chi = u$ in (2.6) and use (2.4)-(2.5) to obtain

$$\frac{1}{2}\frac{d}{dx}\|u\|_{L_2(I_\perp\times\Omega_{\mathbf{v}})}^2 + (\mathbf{v}\cdot\nabla_\perp u, u)_{I_\perp\times\Omega_{\mathbf{v}}} + \frac{1}{2}\|\sigma_{tr}^{1/2}\nabla_{\mathbf{v}} u\|_{L_2(I_\perp\times\Omega_{\mathbf{v}})}^2 = 0, \tag{2.25}$$

where using Green's formula and with $\beta = (\mathbf{v}, 0)$ we have

$$\begin{aligned}(\mathbf{v}\cdot\nabla_\perp u, u)_{I_\perp\times\Omega_{\mathbf{v}}} &= \int_{\Omega_{\mathbf{v}}} \Big(\int_{I_\perp} (\mathbf{v}\cdot\nabla_\perp u) u \Big) dx_\perp\, d\mathbf{v} \\ &= \frac{1}{2}\int_{\Omega_{\mathbf{v}}} (\mathbf{n}\cdot\mathbf{v}) u^2\, d\mathbf{v} = \frac{1}{2}\int_{\Gamma_\beta^+} u^2(\mathbf{n}\cdot\beta)\, d\Gamma \ge 0.\end{aligned} \tag{2.26}$$

Thus

$$\frac{d}{dx}\|u\|_{L_2(I_\perp\times\Omega_{\mathbf{v}})}^2 \le 0, \tag{2.27}$$

which yields (2.23) after integration over $(0,x)$ and taking supremum over $x \in I_x$. Integrating (2.25) over $x \in (0,L)$ and using (2.26) together with the definition of the triple norm $|||\cdot|||_\beta$ we get

$$\|u(L,\cdot,\cdot)\|_{L_2(I_\perp\times\Omega_{\mathbf{v}})}^2 + |||u|||_\beta^2 = \|u(0,\cdot,\cdot)\|_{L_2(I_\perp\times\Omega_{\mathbf{v}})}^2 \tag{2.28}$$

and the estimate (2.24) follows. □

Using the same argument as above we obtain the semi-discrete version of the stability Lemma 2.1:

Corollary 2.2. *The semi-discrete solution u_h with $h = \max(h_\perp, h_{\mathbf{v}})$ and standard Galerkin approximation in phase-space $I_\perp \times \Omega_{\mathbf{v}}$ satisfies the semidiscrete stability estimates:*

$$\sup_{x\in I_x} \|u_h(x,\cdot,\cdot)\|_{L_2(\Omega_\perp\times\Omega_{\mathbf{v}})} \le \|u_{0,h}(\cdot,\cdot)\|_{L_2(\Omega_\perp\times\Omega_{\mathbf{v}})}, \tag{2.29}$$

$$|||u_h|||_\beta \le \|u_{0,h}(\cdot,\cdot)\|_{L_2(\Omega_\perp\times\Omega_{\mathbf{v}})}. \tag{2.30}$$

2.1.2 Convergence

Below we state and prove an a priori error estimate for the finite element approximation u_h satisfying (2.7). The a priori error estimate will be stated in the triple norm defined by (2.22).

Lemma 2.3. *[An a priori error estimate in the triple norm] Assume that u and u_h satisfy the continuous and discrete problems (2.6) and (2.7), respectively. Let $u \in H^r(\Omega) = H^r(\Omega_{\mathbf{x}} \times \Omega_{\mathbf{v}})$, $r \ge 2$, then there is a constant C independent of v, u and h such that*

$$|||u - u_h|||_{\tilde\beta} \le Ch^{r-1/2}\|u\|_{H^r(\Omega)}. \tag{2.31}$$

Proof. Taking the first equations in (2.6) and (2.7) and using (2.5) we end up with

$$\begin{aligned}\Big((u_h-\tilde u)_x,\chi\Big)_{I_\perp\times\Omega_{\mathbf{v}}} + \Big(\mathbf{v}\cdot\nabla_\perp(u_h-\tilde u),\chi\Big)_{I_\perp\times\Omega_{\mathbf{v}}} + \frac{1}{2}\Big(\sigma_{tr}\nabla_{\mathbf{v}}(u_h-\tilde u),\nabla_{\mathbf{v}}\chi\Big)_{I_\perp\times\Omega_{\mathbf{v}}} \\ = \frac{1}{2}\Big(\sigma_{tr}\nabla_{\mathbf{v}}(u-\tilde u),\nabla_{\mathbf{v}}\chi\Big)_{I_\perp\times\Omega_{\mathbf{v}}}.\end{aligned} \tag{2.32}$$

Let now $\chi = u_h - \tilde u$, then by the same argument as in the proof of Lemma 2.1 we get

$$\begin{aligned}\frac{d}{dx}\|u_h-\tilde u\|^2_{L_2(I_\perp\times\Omega_{\mathbf{v}})} + \int_{\Gamma^+_\beta}(\mathbf{n}\cdot\beta)(u_h-\tilde u)^2\,d\Gamma + \|\sigma_{tr}^{1/2}\nabla_{\mathbf{v}}(u_h-\tilde u)\|^2_{L_2(I_\perp\times\Omega_{\mathbf{v}})} \\ \le \frac{1}{2}\|\sigma_{tr}^{1/2}\nabla_{\mathbf{v}}(u_h-\tilde u)\|^2_{L_2(I_\perp\times\Omega_{\mathbf{v}})} + \frac{1}{2}\|\sigma_{tr}^{1/2}\nabla_{\mathbf{v}}(u-\tilde u)\|^2_{L_2(I_\perp\times\Omega_{\mathbf{v}})},\end{aligned} \tag{2.33}$$

which yields

$$\begin{aligned}\frac{d}{dx}\|u_h-\tilde u\|^2_{L_2(I_\perp\times\Omega_{\mathbf{v}})} + \int_{\Gamma^+_\beta}(\mathbf{n}\cdot\beta)(u_h-\tilde u)^2\,d\Gamma + \frac{1}{2}\|\sigma_{tr}^{1/2}\nabla_{\mathbf{v}}(u_h-\tilde u)\|^2_{L_2(I_\perp\times\Omega_{\mathbf{v}})} \\ \le \frac{1}{2}\|\sigma_{tr}^{1/2}\nabla_{\mathbf{v}}(u-\tilde u)\|^2_{L_2(I_\perp\times\Omega_{\mathbf{v}})}.\end{aligned} \tag{2.34}$$

Hence, integrating over $x \in (0, L)$ we obtain

$$\begin{aligned}\|(u_h-\tilde u)(L,\cdot,\cdot)\|^2_{L_2(I_\perp\times\Omega_{\mathbf{v}})} + \int_{\Gamma^+_\beta\setminus\Gamma_L}(\tilde{\mathbf{n}}\cdot\tilde\beta)(u_h-\tilde u)^2\,d\Gamma + \frac{1}{2}\|\sigma_{tr}^{1/2}\nabla_{\mathbf{v}}(u_h-\tilde u)\|^2_{L_2(I_x\times I_\perp\times\Omega_{\mathbf{v}})} \\ \le \frac{1}{2}\|\sigma_{tr}^{1/2}\nabla_{\mathbf{v}}(u-\tilde u)\|^2_{L_2(I_x\times I_\perp\times\Omega_{\mathbf{v}})} + \|(u_h-\tilde u)(0,\cdot,\cdot)\|^2_{L_2(I_\perp\times\Omega_{\mathbf{v}})},\end{aligned} \tag{2.35}$$

where $\Gamma_{\tilde{\beta}}^{+} \setminus \Gamma_L := \{\{L\} \times I_{\perp} \times \Omega_{\mathbf{v}}\}$. Now recalling that $u_h(0,\cdot,\cdot) = \tilde{u}(0,\cdot,\cdot) = u_{0,h}$ and the definition of $|||\cdot|||_{\tilde{\beta}}$ we end up with

$$|||u_h - \tilde{u}|||_{\tilde{\beta}} \leq \|\sigma_{tr}^{1/2} \nabla_{\mathbf{v}}(u - \tilde{u})\|^2_{L_2(I_x \times I_{\perp} \times \Omega_{\mathbf{v}})}. \tag{2.36}$$

Finally using the identity $u_h - u = (u_h - \tilde{u}) + (\tilde{u} - u)$ and the interpolation estimate below we obtain the desired result. □

Proposition 2.4 (See [9]). *Let $h^2 \leq \sigma_{tr}(\mathbf{x}) \leq h$, then there is an interpolation constant $\tilde{C}$ such that*

$$|||u - \tilde{u}|||_{\tilde{\beta}} \leq \tilde{C} h^{r-1/2} \|u\|_r. \tag{2.37}$$

Proof. We rely on classical interpolation error estimates (see [8] and [9]): Let $u \in H^r(\Omega)$, then there exists interpolation constants C_1 and C_2 such that for the nodal interpolant $\pi_h \in \mathcal{V}_{h,\tilde{\beta}}$ of u we have the interpolation error estimates

$$\|u - \pi_h u\|_s \leq C_1 h^{r-s} \|u\|_r, \qquad s = 0,\ 1 \tag{2.38}$$

$$|u - \pi_h u|_{\tilde{\beta}} \leq C_2 h^{r-1/2} \|u\|_r, \tag{2.39}$$

where

$$|\varphi|_{\tilde{\beta}} := \Big(\int_{\Gamma_{\tilde{\beta}}} \varphi^2 (\mathbf{n} \cdot \tilde{\beta})\, d\Gamma \Big)^{1/2}.$$

Using the definition of the triple-norm we have that

$$\begin{aligned} |||u - \pi_h u|||^2_{\tilde{\beta}} =& |u - \pi_h u|^2_{\tilde{\beta}} + \|\sigma_{tr}^{1/2} \nabla_{\mathbf{v}}(u - \pi_h u)\|^2 \\ &\leq |u - \pi_h u|^2_{\tilde{\beta}} + \|\sigma_{tr}^{1/2}\|^2_{\infty} \|u - \pi_h u\|^2_{H^1(\Omega)} \\ &\leq C_2^2 h^{2r-1} \|u\|^2_r + C_1^2 \sup_{\mathbf{x}} |\sigma_{tr}| h^{2r-1} \|u\|^2_r \\ =& \Big(C_2^2 + C_1^2 \sup_{\mathbf{x}} |\sigma_{tr}| \Big) h^{2r-1} \|u\|^2_r \end{aligned} \tag{2.40}$$

where in the last inequality we have used (2.38) and (2.39). Now choosing the constant $\tilde{C} = \Big(C_2^2 + C_1^2 \sup_{\mathbf{x}} |\sigma_{tr}| \Big)^{1/2}$ we get the desired result. □

This proposition yields the L_2 error estimate viz:

Theorem 2.5 (L_2 error estimate). *For $u \in H^r(\Omega)$ and $u_h \in \mathcal{V}_{h,\tilde{\beta}}$ satisfying* (2.6) *and* (2.7), *respectively, and with $h^2 \leq \sigma_{tr} \leq h$, we have that there is a constant $C = C(\Omega, f)$ such that*

$$\|u - u_h\|_{L_2(\Omega)} \leq C h^{r-3/2} \|u\|_r. \tag{2.41}$$

Proof. Using the Poincaré inequality

$$\|u-u_h\|_{L_2(\Omega)} \le C\|\nabla_{\mathbf{v}}(u-u_h)\|_{L_2(\Omega)} \le \frac{C}{\min \sigma_{tr}^{1/2}}\|\sigma_{tr}^{1/2}\nabla_{\mathbf{v}}(u-u_h)\|_{L_2(\Omega)} \tag{2.42}$$

Further using Lemma 2.3

$$\|\sigma_{tr}^{1/2}\nabla_{\mathbf{v}}(u-u_h)\| \le |||u-u_h|||_{\tilde{\beta}} \le Ch^{r-1/2}\|u\|_r. \tag{2.43}$$

Combining (2.42), (2.43) and recalling that σ_{tr} is in the interval $[h^2, h]$ we end up with

$$\|u-u_h\|_{L_2(\Omega)} \le Ch^{r-3/2}\|u\|_r, \tag{2.44}$$

and the proof is complete. □

3 Petrov-Galerkin approaches

Roughly speaking, in the Petrov-Galerkin method one adds a streaming term to the test function. The raison dé etre of such approach is described, motivated and analyzed in the classical SD methods. Here, our objective is to briefly introduce a few cases of Petrov-Galerkin approaches in some lower dimensional geometry and implement them in both direct and adaptive settings. Some specific form of the Petrov-Galerkin methods are studied in [11] where the method of exact transport + projection is introduced. Also both the semi-streamline diffusion as well as the Characteristic streamline diffusion methods, which in their simpler forms are implemented here, are studied in [6].

3.1 A semi-streamline diffusion scheme (SSD)

Here the main difference with the standard approach is that we employ modified test functions of the form $w+\delta\mathbf{v}\cdot\nabla_\perp w$ with $\delta \ge \sigma_{tr}$. Further, we assume that w satisfies the vanishing inflow boundary condition of (1.13). Hence, multiplying the differential equation in (1.13) by $w+\delta(\mathbf{v}\cdot\nabla_\perp w)$ and integrating over $\Omega_\perp = \Omega_{\mathbf{x}_\perp}\times\Omega_{\mathbf{v}}$ we have a variational formulation, viz

$$\begin{aligned}\Big(u_x+\mathbf{v}\cdot\nabla_\perp u-\frac{1}{2}\sigma_{tr}\Delta_{\mathbf{v}}u, w+\delta(\mathbf{v}\cdot\nabla_\perp w)\Big)_\perp &= (u_x,w)_\perp+\delta(u_x,\mathbf{v}\cdot\nabla_\perp w)_\perp+(\mathbf{v}\cdot\nabla_\perp u,w)_\perp\\ &+\delta(\mathbf{v}\cdot\nabla_\perp u,\mathbf{v}\cdot\nabla_\perp w)_\perp+\frac{1}{2}(\sigma_{tr}\nabla_{\mathbf{v}}u,\nabla_{\mathbf{v}}w)_\perp+\frac{\delta}{2}(\sigma_{tr}\nabla_{\mathbf{v}}u,\nabla_{\mathbf{v}}(\mathbf{v}\cdot\nabla_\perp w))_\perp=0.\end{aligned} \tag{3.1}$$

3.1.1 The SSD stability estimate

We let in (3.1) $w=u$ and obtain the following identity

$$\begin{aligned}\frac{1}{2}\frac{d}{dx}\|u\|_\perp^2+\delta(u_x,\mathbf{v}\cdot\nabla_\perp u)_\perp+\frac{1}{2}\int_{\Gamma_\beta^+}(\mathbf{n}\cdot\beta)u^2\,d\Gamma+\delta\|\mathbf{v}\cdot\nabla_\perp u\|_\perp^2\\ +\frac{1}{2}\|\sigma_{tr}^{1/2}\nabla_{\mathbf{v}}u\|_\perp^2+\frac{\delta}{2}\Big(\sigma_{tr}\nabla_{\mathbf{v}}u,\nabla_{\mathbf{v}}(\mathbf{v}\cdot\nabla_\perp u)\Big)_\perp=0.\end{aligned} \tag{3.2}$$

Now it is easy to verify that the last term above can be written as

$$\delta\Big(\sigma_{tr}\nabla_{\mathbf{v}}u,\nabla_{\mathbf{v}}(\mathbf{v}\cdot\nabla_{\perp}u)\Big)_{\perp}=\delta\int_{\Omega_{\perp}}\sigma_{tr}\Big(\nabla_{\mathbf{v}}u\cdot\nabla_{\perp}u+\frac{1}{2}\mathbf{v}\cdot\nabla_{\perp}(|\nabla_{\mathbf{v}}u|)^2\Big)\,dx_{\perp}\,d\mathbf{v}. \tag{3.3}$$

Due to symmetry the second term in the integral above vanishes. Hence we end up with

$$\begin{aligned}\frac{1}{2}\frac{d}{dx}\|u\|_{\perp}^2+\delta(u_x,\mathbf{v}\cdot\nabla_{\perp}u)_{\perp}+\frac{1}{2}\int_{\Gamma_{\beta}^{+}}(\mathbf{n}\cdot\beta)u^2\,d\Gamma+\delta\|\mathbf{v}\cdot\nabla_{\perp}u\|_{\perp}^2\\+\frac{1}{2}\|\sigma_{tr}^{1/2}\nabla_{\mathbf{v}}u\|_{\perp}^2+\frac{\delta}{2}\Big(\sigma_{tr}\nabla_{\mathbf{v}}u,\nabla_{\perp}u)\Big)_{\perp}=0.\end{aligned} \tag{3.4}$$

Next, we multiply the differential equation (1.13) by δu_x and integrate over $I_{\perp}\times\Omega_{\mathbf{v}}$ to get

$$\delta\|u_x\|^2+(\delta u_x,\mathbf{v}\cdot\nabla_{\perp}u)_{\perp}+\frac{\delta}{2}(\sigma_{tr}\nabla_{\mathbf{v}}u,\nabla_{\mathbf{v}}u_x)_{\perp}=0. \tag{3.5}$$

The last inner product on the left hand side of (3.5) can be written as

$$(\sigma_{tr}\nabla_{\mathbf{v}}u,\nabla_{\mathbf{v}}u_x)_{\perp}=\frac{1}{2}\frac{d}{dx}\int_{I_{\perp}\times\Omega_{\mathbf{v}}}\sigma_{tr}|\nabla_{\mathbf{v}}|^2\,dx_{\perp}\,d\mathbf{v}-\frac{1}{2}\int_{I_{\perp}\times\Omega_{\mathbf{v}}}\frac{\partial\sigma_{tr}}{\partial x}\Big(|\nabla_{\mathbf{v}}|^2\Big)\,dx_{\perp}\,d\mathbf{v}. \tag{3.6}$$

Now inserting (3.6) in (3.5) and adding the result to (3.4) we end up with

$$\begin{aligned}\frac{1}{2}\frac{d}{dx}\|u\|_{\perp}^2+\delta\|u_x+\mathbf{v}\cdot\nabla_{\perp}u\|_{\perp}^2+\frac{1}{2}\int_{\Gamma_{\beta}^{+}}(\mathbf{n}\cdot\beta)u^2\,d\Gamma+\frac{1}{2}\|\sigma_{tr}^{1/2}\nabla_{\mathbf{v}}u\|_{\perp}^2\\+\frac{\delta}{2}\Big(\sigma_{tr}\nabla_{\mathbf{v}}u,\nabla_{\perp}u\Big)_{\perp}+\frac{\delta}{4}\frac{d}{dx}\int_{I_{\perp}\times\Omega_{\mathbf{v}}}\sigma_{tr}|\nabla_{\mathbf{v}}|^2\,dx_{\perp}\,d\mathbf{v}\\-\frac{\delta}{4}\int_{I_{\perp}\times\Omega_{\mathbf{v}}}\frac{\partial\sigma_{tr}}{\partial x}\Big(|\nabla_{\mathbf{v}}|^2\Big)\,dx_{\perp}\,d\mathbf{v}=0.\end{aligned} \tag{3.7}$$

Further we use the Cauchy-Schwarz inequality to get

$$|\Big(\sigma_{tr}\nabla_{\mathbf{v}}u,\nabla_{\perp}u\Big)_{\perp}|\leq\frac{1}{2}\|\sigma_{tr}^{1/2}\nabla_{\perp}u\|_{\perp}^2+\frac{1}{2}\|\sigma_{tr}^{1/2}\nabla_{\mathbf{v}}u\|_{\perp}^2. \tag{3.8}$$

Finally with an additional symmetry assumption on $x_{\perp}$ and $\mathbf{v}$ convections as (this is motivated by forward peakedness assumption in angle and energy which is used in deriving the Fokker-Plank/Fermi equations)

$$\|\sigma_{tr}^{1/2}\nabla_{\perp}u\|_{\perp}\sim\|\sigma_{tr}^{1/2}\nabla_{\mathbf{v}}u\|_{\perp}, \tag{3.9}$$

and the fact that σ_{tr} is decreasing in the beams penetration direction, i.e. $\frac{\partial\sigma_{tr}}{\partial x}\leq 0$, we may write (3.7) as

$$\begin{aligned}\frac{1}{2}\frac{d}{dx}\Big(\|u\|_{\perp}^2+\frac{1}{2}\delta\int_{I_{\perp}\times\Omega_{\mathbf{v}}}\sigma_{tr}|\nabla_{\mathbf{v}}|^2\,dx_{\perp}\,d\mathbf{v}\Big)+\frac{1}{2}\int_{\Gamma_{\beta}^{+}}(\mathbf{n}\cdot\beta)u^2\,d\Gamma+\delta\|u_x+\mathbf{v}\cdot\nabla_{\perp}u\|_{\perp}^2\\+\frac{1}{2}(1-\delta)\|\sigma_{tr}^{1/2}\nabla_{\mathbf{v}}u\|_{\perp}^2\leq 0.\end{aligned} \tag{3.10}$$

As a consequence for sufficiently small δ (actually $\delta \approx \sigma_{tr}^{1/2} \ll 1$) we have, e.g.

$$\frac{d}{dx}\Big(\|u\|_{\perp}^2 + \frac{1}{2}\delta \int_{I_\perp \times \Omega_{\mathbf{v}}} \sigma_{tr} |\nabla_{\mathbf{v}}|^2 \, dx_\perp \, d\mathbf{v}\Big) < 0, \tag{3.11}$$

and hence $\|u\|_{\perp}^2 + \frac{\delta}{2}\int_{I_\perp \times \Omega_{\mathbf{v}}} \sigma_{tr}|\nabla_{\mathbf{v}}|^2 \, dx_\perp \, d\mathbf{v}$ is strictly decreasing in x. Consequently, for each $x' \in [0, L]$ we have that

$$\|u(x', \cdot, \cdot)\|_{\perp}^2 + \frac{\delta}{2}\|\sigma_{tr}^{1/2}\nabla_{\mathbf{v}} u(x', \cdot, \cdot)\|_{\perp}^2 \leq \|u(0, \cdot, \cdot)\|_{L_2(I_\perp \times \Omega_{\mathbf{v}})}^2 + \frac{\delta}{2}\|\sigma_{tr}^{1/2}\nabla_{\mathbf{v}} u(0, \cdot, \cdot)\|_{\perp}^2. \tag{3.12}$$

Thus, summing up we have proved the following stability estimates

Proposition 3.1. *Under the assumption* (3.9) *the following* $L_2(I_\perp \times \Omega_{\mathbf{v}})$ *stability holds true*

$$\|u(L, \cdot, \cdot)\|_{\perp}^2 + \frac{\delta}{2}\|\sigma_{tr}^{1/2}\nabla_{\mathbf{v}} u(L, \cdot, \cdot)\|_{\perp}^2 \leq \|u_0\|_{\perp}^2 + \frac{\delta}{2}\|\sigma_{tr}^{1/2}\nabla_{\mathbf{v}} u_0\|_{\perp}^2. \tag{3.13}$$

Moreover, we have also the second stability estimate

$$|||u|||_{\tilde{\beta}}^2 + \delta\|u_x + \mathbf{v}\cdot\nabla_\perp u\|_{L_2(\Omega)}^2 \leq \tilde{C}\Big(\|u_0\|_{L_2(I_\perp \times \Omega_{\mathbf{v}})}^2 + \delta\|\sigma_{tr}^{1/2}\nabla_{\mathbf{v}} u_0\|_{L_2(I_\perp \times \Omega_{\mathbf{v}})}^2\Big). \tag{3.14}$$

Remark 3.2. Due to the size of smallness parameters δ and σ_{tr} we can easily verify the second stability estimate (3.14) which also yields

$$\|u_x + \mathbf{v}\cdot\nabla_\perp u\|_{L_2(\Omega)} \leq \tilde{C}\|\sigma_{tr}^{1/2}\nabla_{\mathbf{v}} u_0\|_{L_2(I_\perp \times \Omega_{\mathbf{v}})}. \tag{3.15}$$

Hence, using the equation (1.13), we get

$$\|\sigma_{tr}\Delta_{\mathbf{v}} u\|_{L_2(\Omega)} \leq \tilde{C}\|\sigma_{tr}^{1/2}\nabla_{\mathbf{v}} u_0\|_{L_2(I_\perp \times \Omega_{\mathbf{v}})}. \tag{3.16}$$

The estimate (3.16) indicates the regularizing effect of the diffusive term $\Delta_{\mathbf{v}} u$ in the sense that $u_0 \in H^r_{\sqrt{\sigma_{tr}}}(I_\perp \times \Omega_{\mathbf{v}})$ implies that $u \in H^{r+1}_{\sigma_{tr}}(I_\perp \times \Omega_{\mathbf{v}})$. However this regularizing effect will decrease by the size of σ_{tr}.

4 Model problems in lower dimensions

We consider now a forward peaked narrow radiation beam entering into the symmetric domain $I_y \times I_\eta = [-y_0, y_0] \times [-\eta_0, \eta_0]$; $(y_0, \eta_0) \in \mathbb{R}_+^2$ at $(0, 0)$ and penetrating in the direction of the positive x-axis. Then the computational domain Ω of our study is a three dimensional slab with $(x, y, \eta) \in \Omega = I_x \times I_y \times I_\eta$ where $I_x = [0, L]$. In this way, the problem (1.13) will be transformed into the following lower dimensional model problem

$$\begin{cases} u_x + \eta u_y = \frac{1}{2}\sigma_{tr} u_{\eta\eta} & (x, y, \eta) \in \Omega, \\ u_\eta(x, y, \pm\eta_0) = 0 & (x, y) \in I_x \times I_y, \\ u(0, y, \eta) = f(y, \eta) & (y, \eta) \in I_y \times I_\eta, \\ u(x, y, \eta) = 0 & \text{on } \Gamma_\beta^- \setminus \{(0, y, \eta)\}. \end{cases} \tag{4.1}$$

For this problem we implement two different versions of the streamline diffusion method: the semi-streamline diffusion and the characteristic streamline diffusion. Both cases are discretized using linear polynomial approximations.

4.1 The semi-streamline diffusion method

In this version we derive a discrete scheme for computing the approximate solution u_h of the exact solution u using the SD-method for discretizing the (y,η)-variables (corresponding to multiply the equation by test functions of the form $w+\delta\eta w_y$) combined with the backward Euler method for the x-variable. We start by introducing the bilinear forms $a(\cdot,\cdot)$ and $b(\cdot,\cdot)$ for the problem (4.1) as:

$$\begin{aligned} a(u,w) =& (\eta u_y, w)_\perp + \delta(\eta u_y, \eta w_y)_\perp + \frac{1}{2}(\sigma_{tr} u_\eta, w_\eta)_\perp \\ &+ \frac{1}{2}\delta(\sigma_{tr} u_\eta, w_y + \eta w_{y\eta})_\perp - \frac{1}{2}\delta \int_{I_y} \sigma_{tr}\eta u_\eta w_y \Big|_{\eta=-\eta_0}^{\eta=\eta_0} dy, \\ b(u,w) =& (u,w)_\perp + \delta(u, \eta w_y)_\perp, \end{aligned} \tag{4.2}$$

where $(\cdot,\cdot)_\perp := (\cdot,\cdot)_{I_y\times I_\eta}$. Then the continuous problem reads as: for each $x\in(0,L]$, find $u(x,\cdot)\in H^1_\beta$ such that

$$b(u_x,w)+a(u,w)=0, \qquad \forall w\in H^1_\beta,$$

where

$$H^1_\beta := \{w\in H^1(I_y\times I_\eta); w=0 \text{ on } \Gamma^-_\beta\},$$

and

$$\Gamma^-_\beta := \{(y,\eta)\in\Gamma := \partial(I_y\times I_\eta), \text{ with } \mathbf{n}\cdot\beta<0\}, \tag{4.3}$$

with $\beta=(\eta,0)$. Then the semi-streamline diffusion method for the continuous problem (4.1) reads as follows: for each $x\in(0,L]$, find $u_h(x,\cdot)\in\mathcal{V}_{h,\beta}$ such that,

$$b(u_{h,x},w)+a(u_h,w)=0, \quad \forall w\in\mathcal{V}_{h,\beta}, \tag{4.4}$$

where $\mathcal{V}_{h,\beta}\subset H^1_\beta$ consists of continuous piecewise linear functions. Next, we write the global discrete solution by separation of variables as

$$u_h(x,y,\eta)=\sum_{j=1}^{N} U_j(x)\phi_j(y,\eta), \tag{4.5}$$

where N is the number of nodes in the mesh. Letting $w=\phi_i$ for $i=1,2,\ldots,N$ and inserting (4.5) into (4.4) we get the following discrete system of equations,

$$\sum_{j=1}^{N} U_j'(x)b(\phi_j,\phi_i)+\sum_{j=1}^{N} U_j(x)a(\phi_j,\phi_i)=0, \quad i=1,2,\ldots,N. \tag{4.6}$$

Equation (4.6) in matrix form can be written as

$$BU'(x)+AU(x)=0, \tag{4.7}$$

with $U = [U_1, ..., U_N]^T, B = (b_{ij}), b_{ij} = b(\phi_j, \phi_i)$ and $A = (a_{ij}), a_{ij} = a(\phi_j, \phi_i), i, j = 1, 2, \ldots, N$. We apply now the backward Euler method for further discretization of the equation (4.7) in variable x, and with the step size k_m, to obtain an iterative form viz

$$B(U^{m+1} - U^m) + k_m A U^{m+1} = 0. \tag{4.8}$$

The equation above can be rewritten as a system of equations for finding the solution U^{m+1} (at "time" level $x = x_{m+1}$) on iteration $m+1$ from the known solution U^m from the previous iteration step m:

$$[B + k_m A]U^{m+1} = BU^m. \tag{4.9}$$

4.2 Characteristic Streamline Diffusion Method

In this part we construct an oriented phase-space mesh to obtain the characteristic streamline diffusion method. Before formulating this method, we need to construct a new subdivision of $\Omega = I_x \times I_y \times I_\eta$. To this end and for $m = 1, 2, \ldots, M$, we define a subdivision of $\Omega_m = [x_{m-1}, x_m] \times I_y \times I_\eta := I_m \times I_y \times I_\eta$ into elements

$$\hat{\tau}_m = \{(x, y + (x - x_m)\eta, \eta) : (y, \eta) \in \tau \in \mathcal{T}_h,\ x \in I_m\},$$

where $\mathcal{T}_h$ is a previous triangulation of $I_\perp$. Then we introduce, *slabwise*, the function spaces

$$\hat{\mathcal{V}}_m = \{\hat{w} \in C(\Omega_m) : \hat{w}(x, y, \eta) = w(y + (x - x_m)\eta, \eta), w \in \mathcal{V}_{h,\beta}\}.$$

In other words $\hat{\mathcal{V}}_m$ consists of continuous functions $\hat{w}(x, y, \eta)$ on Ω_m such that $\hat{w}$ is constant along characteristics $(\hat{y}, \hat{\eta}) = (y + x\eta, \eta)$ parallel to the sides of the elements $\hat{\tau}_m$, meaning that the derivative in the characteristic direction: $\hat{w}_x + \eta \hat{w}_y = 0$. The streamline diffusion method can now be reduced to the following formulation (where only the σ_{tr}-term survives): find $\hat{u}_h$ such that, for each $m = 1, 2, \ldots, M$, $\hat{u}_h|_{\Omega_m} \in \hat{\mathcal{V}}_m$ and

$$\begin{aligned} \frac{1}{2} \int_{\Omega_m} \sigma_{tr} \hat{u}_{h,\eta} w_\eta \, dxdyd\eta + \int_{I_\perp} \hat{u}_{h,+}(x_{m-1}, y, \eta) w_+(x_{m-1}, y, \eta) \, dyd\eta \\ = \int_{I_\perp} \hat{u}_{h,-}(x_{m-1}, y, \eta) w_+(x_{m-1}, y, \eta) \, dyd\eta, \quad \forall w \in \hat{\mathcal{V}}_m. \end{aligned} \tag{4.10}$$

Here, for definition of $\hat{u}_{h,+}, \hat{u}_{h,-}, w_+$ we refer to (2.12).

5 Adaptive algorithm

In this section we formulate an adaptive algorithm, which is used in computations of the numerical examples studied in Section 6. This algorithm improves the accuracy of the computed solution u_h of the model problem (4.1). In the sequel for simplicity we denote $I_y \times I_\eta$ also by $\Omega_\perp$ (this however, should not be mixed with the notation in the theoretical Sections 1-3).

Nr. of refinement, n	Nr. of elements	Nr. of vertices	DOF	$e_n = \|u - u_h^n\|_{L_2}$	e_n/e_{n+1}
0	272	157	157	8.364e-03	
1	1176	591	591	2.134e-04	3.92
2	4704	2268	2268	5.368e-04	3.97
3	17616	8878	8878	1.345e-05	3.99
4	69864	35231	35231	1.263e-05	4.00

Table 1: Test 1-a). Computed errors $e_n = \|u - u_h^n\|_{L_2(\Omega_\perp)}$ and e_n/e_{n+1} on the adaptively refined meshes. Here, the solution u_h^n is computed using semi-streamline diffusion method of section 4.1 with $\widetilde{\gamma} = 0.5$ in the adaptive algorithm and $\alpha = 0.1$ in (6.2).

The Mesh Refinement Recommendation *We refine the mesh in neighborhoods of those points in $I_y \times I_\eta$ where the error $\varepsilon_n = |u - u_h^n|$ attains its maximal values. More specifically, we refine the mesh in such subdomains of $I_y \times I_\eta$ where*

$$\varepsilon_n \geq \widetilde{\gamma} \max_{\Omega_\perp} \varepsilon_n.$$

Here $\widetilde{\gamma} \in (0, 1)$ is a number which should be chosen computationally and u_h^n denotes the computed solution on the n-th refinement of the mesh.

The steps in adaptive algorithm

Step 0. Choose an initial mesh $I_m^0 \times \tau^0$ in $I_x \times I_y \times I_\eta$ and obtain the numerical solution u_h^n, $n > 0$, where n is number of the mesh refinements, in the following steps:

Step 1. Compute the numerical solution u_h^n on τ^n using any of the finite element methods introduced in section 4.

Step 2. Refine those elements in the mesh τ^n for which

$$\varepsilon_n \geq \widetilde{\gamma} \max_{\Omega_\perp} \varepsilon_n. \tag{5.1}$$

Here, the values for the tolerance $\widetilde{\gamma} \in (0, 1)$ are chosen by the user.

Step 3. Define a new refined mesh as τ^{n+1}. Construct a new partition I_m^{n+1} if needed. Perform steps 1-3 on the mesh $I_m^{n+1} \times \tau^{n+1}$. Stop mesh refinements when $\|u_h^n - u_h^{n-1}\|_{L_2(\Omega_\perp)} < tol$, where *tol* is a total tolerance chosen by the user.

Nr. of refinement, n	Nr. of elements	Nr. of vertices	DOF	$e_n = \|u - u_h^n\|_{L_2}$	e_n/e_{n+1}
0	272	157	157	8.364e-03	
1	1088	585	585	8.278e-03	1.01
2	4352	2257	2257	2.105e-03	3.93
3	17408	8865	8865	5.290e-04	3.98
4	69632	35137	35137	1.325e-04	3.99

Table 2: Test 1-b). Computed errors $e_n = \|u - u_h^n\|_{L_2(\Omega_\perp)}$ and e_n/e_{n+1} on the adaptively refined meshes. Here, the solution u_h^n is computed using semi-streamline diffusion method of section 4.1 with $\widetilde{\gamma} = 0.7$ in the adaptive algorithm and $\alpha = 0.1$ in (6.2).

6 Numerical examples

In this section we present numerical examples which show the performance of an adaptive finite element method for the solution of the model problem (4.1). Here, all computations are performed in Matlab COMSOL Multiphysics using module LIVE LINK MATLAB. We choose the domain $\Omega_\perp = I_y \times I_\eta$ as

$$\Omega_\perp = \{(y, \eta) \in (-1.0, 1.0) \times (-1.0, 1.0)\}.$$

Our tests are performed with a fixed diffusion coefficient $\sigma_{tr} = 0.002$. Further, due to smallness of the parameters δ and σ_{tr}, the terms that involve the product $\delta\sigma_{tr}$ are assumed to be negligible. In the backward Euler scheme, used discretization in x-variable, we solve the system of equations (4.9) which ends up with a discrete (computed) solution U^{m+1} of (4.1) at the time iteration $m + 1$ and with the time step k_m which has been chosen to be $k_m = 0.01$.

Previous computational studies, e.g. [3], have shown oscillatory behavior of the solution u_h when the semi-streamline diffusion method was used, and layer behavior when the standard Galerkin method was applied to solve the model problem (4.1). In this work we significantly improve results of [3] by using the adaptive algorithm of section 5 on the locally adaptively refined meshes. All our computations are compared with the closed form analytic solution for the model problem (4.1) given by

$$u(x, y, \eta) = \frac{\sqrt{3}}{\pi\sigma_{tr}x^2} \exp\left[-\frac{2}{\sigma_{tr}}\left(\frac{3y^2}{x^3} - \frac{3y\eta}{x^2} + \frac{\eta^2}{x}\right)\right], \tag{6.1}$$

when the initial data is given by $u(0, y, \eta) = \delta(y)\delta(\eta)$.

We have performed the following computational tests:

- Test 1. Solution of the model problem (4.1) with a "Dirac type" initial condition

$$u(0, y, \eta) = f(y, \eta) = 1/(y^2 + \eta^2 + \alpha), \quad (y, \eta) \in \Omega_\perp, \tag{6.2}$$

  for different values of the parameter $\alpha \in (0, 1)$.

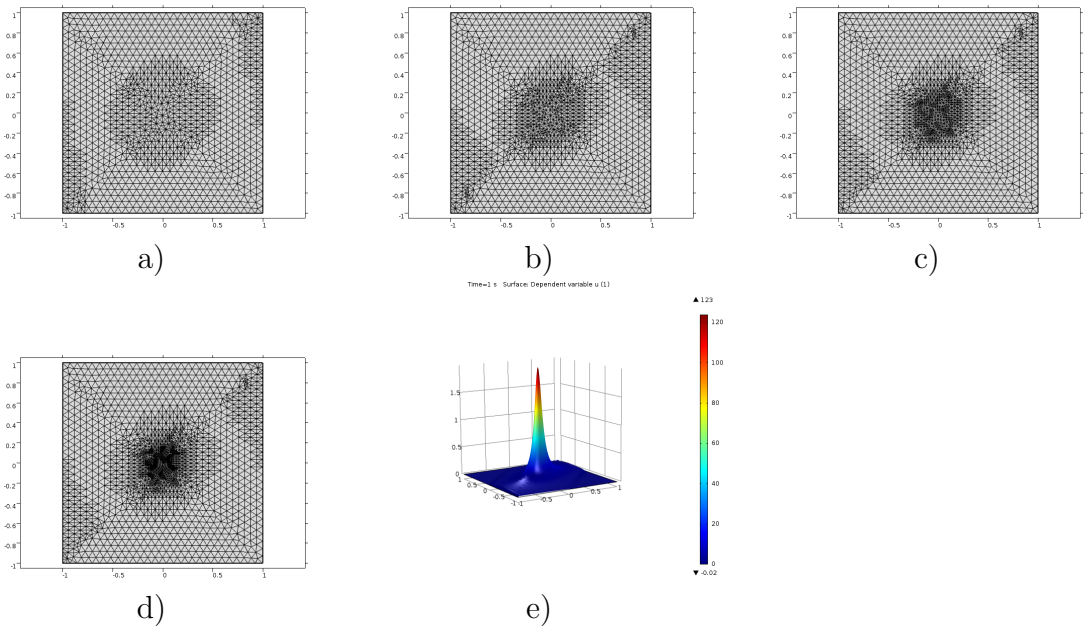

Figure 1: Test 1-a. a)-d) Locally adaptively refined meshes of Table 1; e) Computed solution on the 4 times adaptively refined mesh d).

- Test 2. Solution of the model problem (4.1) with "Maxwellian type" initial condition

$$u(0, y, \eta) = f(y, \eta) = \exp^{-(y^2+\eta^2+\alpha)}, \quad (y, \eta) \in \Omega_{\perp}, \tag{6.3}$$

  for different values of $\alpha \in (0, 1)$.

- Test 3. Solution of the model problem (4.1) with a "hyperbolic type" initial condition

$$u(0, y, \eta) = f(y, \eta) = \frac{1}{\sqrt{y^2 + \eta^2 + \alpha}}, \quad (y, \eta) \in \Omega_{\perp}, \tag{6.4}$$

  for $\alpha = 0.19$.

6.1 Test 1

In this test we compute numerical simulations for the problem (4.1) with a "Dirac type" initial condition (6.2) and for different values of the parameter $\alpha \in (0, 1)$ in (6.2), where we use adaptive algorithm of Section 4 on the locally adaptively refined meshes. These meshes were refined according to the error indicator (5.1) in the adaptive algorithm. For computation of the finite element solution we employ semi-streamline diffusion method of Section 4.1. We performed two set of numerical experiments:

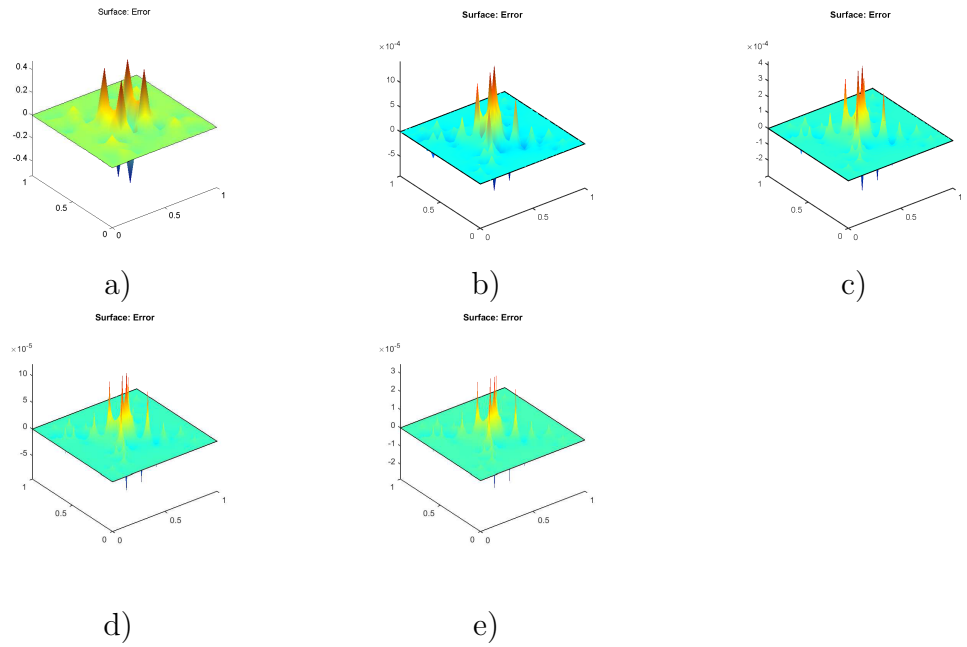

Figure 2: Test 1-a). Computed errors $\mathcal{E}_n(x,y) = u(x,y) - u_h^n(x,y)$ on the locally adaptively refined meshes of Table 1 on the meshes of Figure 1-a)-d).

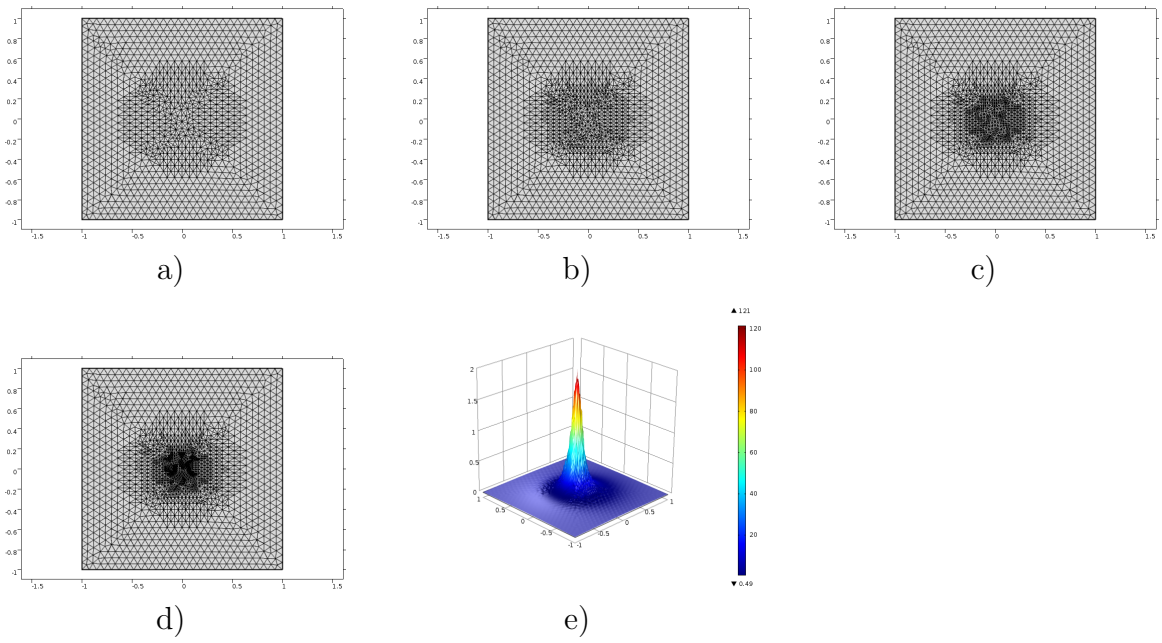

Figure 3: Test 1-b. a)-d) Locally adaptively refined meshes of Table 2; e) Computed solution on the 4 times adaptively refined mesh d).

Nr. of refinement, n	Nr. of elements	Nr. of vertices	DOF	$e_n = \|u - u_h^n\|_{L_2}$	e_n/e_{n+1}
0	272	157	585	2.582e-04	
1	1288	592	2267	3.242e-05	7.97
2	4552	2267	8911	4.062e-06	7.98
3	17628	8911	35432	5.085e-07	7.99
4	69812	35432	141612	4.362e-07	7.99

Table 3: Test 2-a). Computed values of errors $e_n = \|u - u_h^n\|_{L_2(\Omega_\perp)}$ and e_n/e_{n+1} on the adaptively refined meshes. Here, the solution u_h^n is computed using characteristic streamline diffusion method with $\widetilde{\gamma} = 0.5$ in the adaptive algorithm.

- Test 1-a). We take $\widetilde{\gamma} = 0.5$ in (5.1). This choice of the parameter allows to refine the mesh τ not only at the center of the domain $\Omega_\perp$, but also at the boundaries of $\Omega_\perp$.
- Test 1-b). We take $\widetilde{\gamma} = 0.7$ in (5.1). Such choice of the parameter allows to refine the mesh τ only at the middle of the domain $\Omega_\perp$.

Our computational tests have shown that the values for $\alpha \in (0.05, 0.1)$ give smaller computational errors $e_n = \|u - u_h^n\|_{L_2(\Omega_\perp)}$ than the other α-values. The results of the computations for $\alpha = 0.1$ are presented in Tables 1 and 2 for Test 1-a) and Test 1-b), respectively. Using these tables and Figures 1 and 3 we observe that we have obtained significant reduction of the computational error $e_n = \|u - u_h^n\|_{L_2(\Omega_\perp)}$ on the adaptively refined meshes. These errors in the form $\mathcal{E}_n(x, y) = u(x, y) - u_h^n(x, y)$, on the adaptively refined meshes, are shown on Figure 2. Using Tables 1, 2 we observe that the reduction of the computational error is faster and more significant in the case a) than in the case b). Thus, choosing the parameter $\widetilde{\gamma} = 0.5$ in (5.1) gives a better computational result and smaller error e_n than $\widetilde{\gamma} = 0.7$. This allows us to conclude that the refinement of the mesh τ not only at the center of the domain $\Omega_\perp$, but also at the boundaries of $\Omega_\perp$ give significantly smaller computational error $e_n = \|u - u_h^n\|_{L_2(\Omega_\perp)}$.

We present the final solution u_h^4 computed on the 4 times adaptively refined mesh on the Figure 1-f) for Test 1-a) and on the Figure 3-f) for Test 1-b). We note that in both cases we have obtained smoother computed solution u_h^4 without any oscillatory behavior. This is a significant improvement of the result of [3] where mainly oscillatory solution could be obtained.

6.2 Test 2

In this test we perform numerical simulations for the problem (4.1) with Maxwellian initial condition (6.3) and for different values of the parameter $\alpha \in (0, 1)$. Again we use the error indicator (5.1) in the adaptive algorithm for local refinement of meshes and perform two set of tests as in the case of Test 1 and with the same values on the parameter $\widetilde{\gamma}$.

Nr. of refinement, n	Nr. of elements	Nr. of vertices	DOF	$e_n = \|u - u_h^n\|_{L_2}$	e_n/e_{n+1}
0	272	157	585	2.582e-03	
1	1088	585	2257	2.706e-03	7.81
2	4352	2257	8865	3.427e-04	7.90
3	17408	8865	35137	4.307e-05	7.96
4	69632	35137	139905	5.398e-06	7.98

Table 4: Test 2-b). Computed values of errors $e_n = \|u - u_h^n\|_{L_2(\Omega_\perp)}$ and e_n/e_{n+1} on the adaptively refined meshes. Here, the solution u_h^n is computed using characteristic streamline diffusion method with $\widetilde{\gamma} = 0.7$ in the adaptive algorithm.

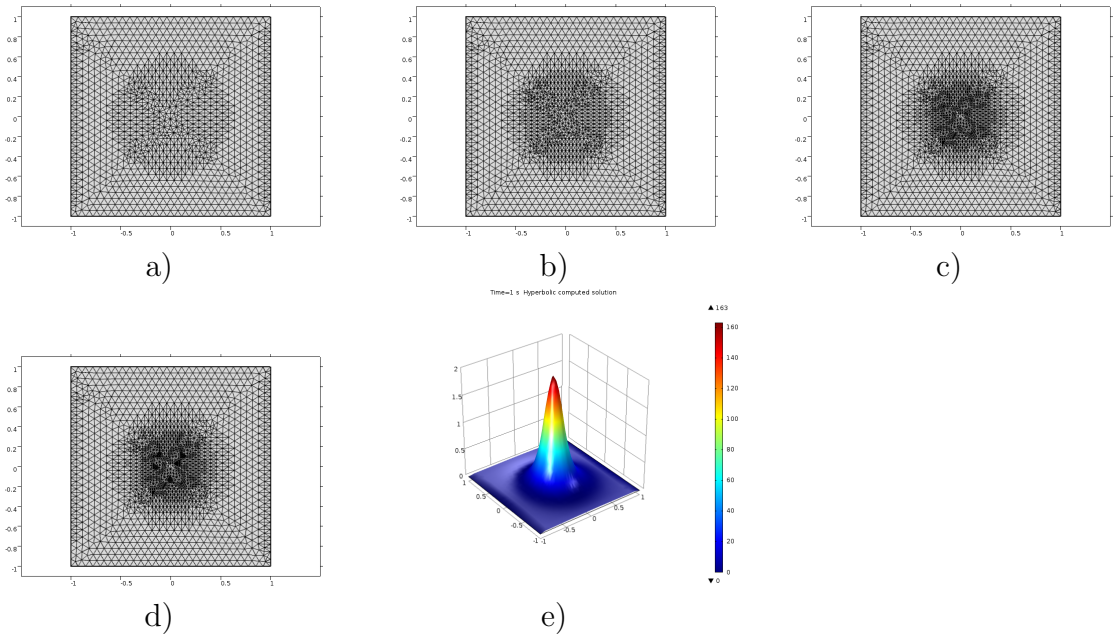

Figure 4: Test 2-a). a)-d) Locally adaptively refined meshes of Table 3; e) Computed solution on the 4 times adaptively refined mesh d).

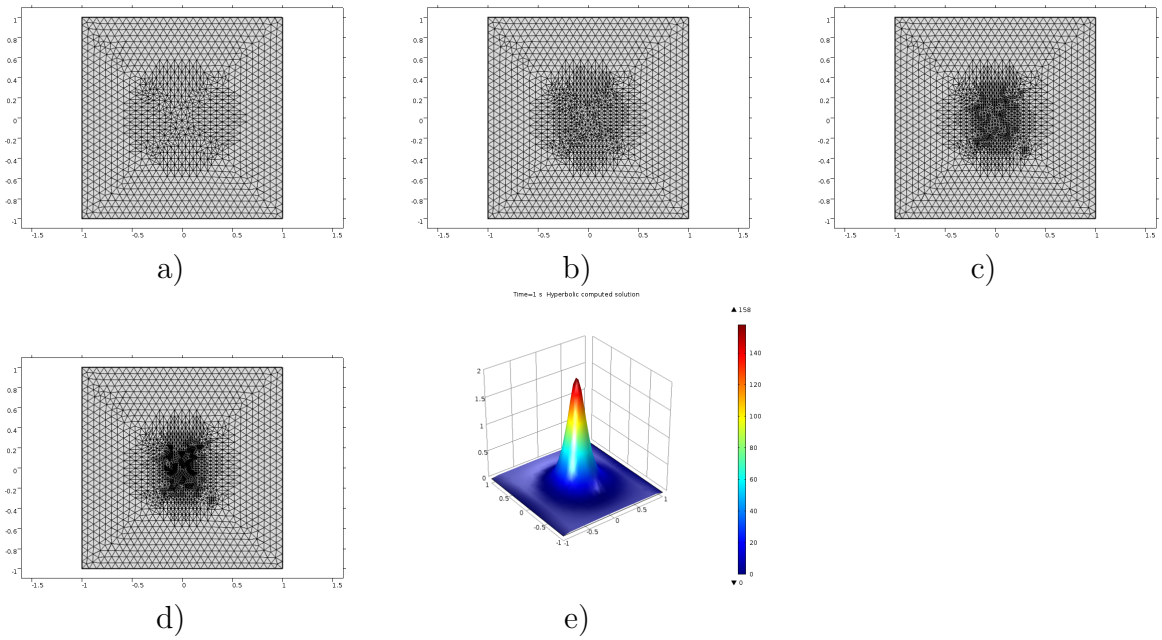

Figure 5: Test 2-b). a)-d) Locally adaptively refined meshes of Table 4; e) Computed solution on the 4 times adaptively refined mesh d).

For finite element discretization we use semi-streamline diffusion method as in the Test 1. To be able to control the formation of the layer which appears at the central point $(y, \eta) = (0, 0)$ we use different values of $\alpha \in (0, 1)$ inside the function (6.3). Our computational tests show that the value of the parameter $\alpha = 0.19$ is optimal one.

We present results of our computations for $\alpha = 0.19$ in Tables 3 and 4 for Test 2-a) and Test 2-b), respectively. Using these Tables and Figures 4 and 5, once again, we observe significant reduction of the computational error $e_n = \|u - u_h^n\|_{L_2(\Omega_\perp)}$ on the adaptively refined meshes. Using Tables 3 and 4 again we observe more significant reduction of the computational error in the case a) then in the case b). Thus, choosing the parameter $\widetilde{\gamma} = 0.5$ in (5.1) yields better computational results.

Final solution u_h^4 computed on the 4 times adaptively refined mesh is shown on the Figure 4-f) for Test 2-a) and on the Figure 5-f) for Test 2-b). Again we observe that, with the above numerical values for the parameters, α and $\widetilde{\gamma}$ we have avoided the formation of layers and in both tests we have obtained smooth computed solution u_h^4.

6.3 Test 3

In this test we perform numerical simulations of the problem (4.1) with hyperbolic initial condition (6.4) on the locally adaptively refined meshes. Taking into account results of our previous Tests 1,2 we take fixed value of $\alpha = 0.19$ in (6.4). For finite element discretization we used the semi-streamline diffusion method of Section 4. We again perform two set of

Nr. of refinement, n	Nr. of elements	Nr. of vertices	DOF	$e_n = \|u - u_h^n\|_{L_2}$	e_n/e_{n+1}
0	272	157	1285	1.565e-05	
1	1271	597	5115	9.732e-07	16.08
2	5084	2267	20937	6.052e-08	16.08
3	20336	9075	79825	3.771e-09	16.05

Table 5: Test 3-a). Computed values of errors $e_n = \|u - u_h^n\|_{L_2(\Omega_\perp)}$ and e_n/e_{n+1} on the adaptively refined meshes. Here, the solution u_h^n is computed using semi-streamline diffusion method with $\widetilde{\gamma} = 0.5$ in the adaptive algorithm.

Nr. of refinement, n	Nr. of elements	Nr. of vertices	DOF	$e_n = \|u - u_h^n\|_{L_2}$	e_n/e_{n+1}
0	272	157	1285	1.565e-05	
1	1088	585	5017	1.484e-06	15.98
2	4352	2257	19825	9.289e-07	16.02
3	17408	8865	78817	5.799e-08	16.02

Table 6: Test 3-b). Computed values of errors $e_n = \|u - u_h^n\|_{L_2(\Omega_\perp)}$ and e_n/e_{n+1} on the adaptively refined meshes. Here, the solution u_h^n is computed using semi-streamline diffusion method with $\widetilde{\gamma} = 0.7$ in the adaptive algorithm.

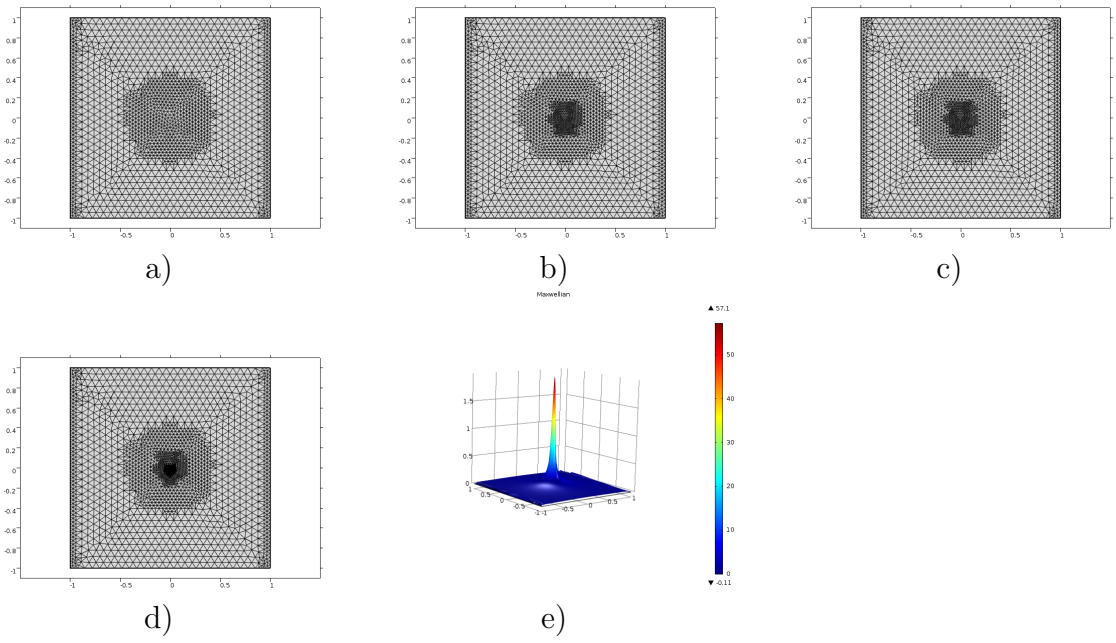

Figure 6: Test 3-a). a)-d) Locally adaptively refined meshes of Table 5; e) Computed solution on the 4 times adaptively refined mesh d).

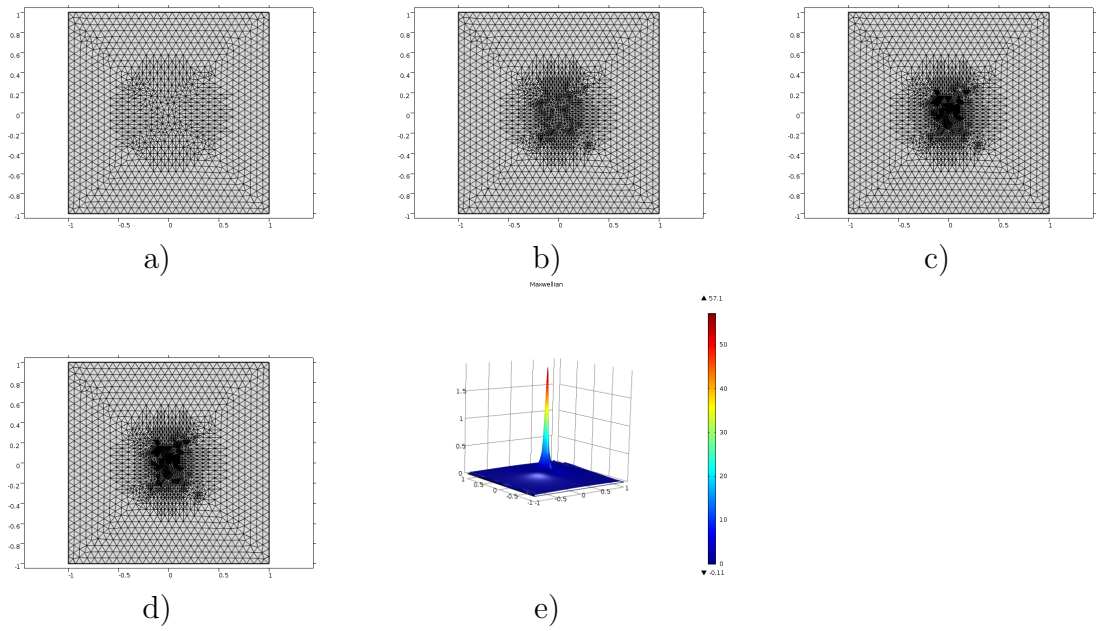

Figure 7: Test 3-b). a)-d) Locally adaptively refined meshes of Table 6; e) Computed solution on the 4 times adaptively refined mesh d).

tests with different values of $\tilde{\gamma}$ in (5.1): in the Test 3-a) we choose $\tilde{\gamma} = 0.5$, and in the Test 3-b) we assign this parameter to be $\tilde{\gamma} = 0.7$.

We present results of our computations in Tables 5 and 6. Using these tables and Figures 6 and 7 we observe significant reduction of the computational error $e_n = \|u - u_h^n\|_{L_2(\Omega_\perp)}$ on the adaptively refined meshes. Final solutions u_h^4 computed on the 4 times adaptively refined meshes are shown on the Figure 6-f) for the Test 3-a) and on the Figure 7-f) for the Test 3-b), respectively.

7 Conclusion

Finite element method (FEM) is commonly used as numerical method for solution of PDEs. In this work FEM is applied to compute approximate solution of a, *degenerate type*, convection dominated convection-diffusion problem. We consider linear polynomial approximations and study different finite element discretizations for the solutions for pencil-beam models based on Fermi and Fokker-Planck equations. First we have derived stability estimates and proved optimal convergence rates (due to the maximal available regularity of the exact solution) in a more general setting in physical domain. Then we have specified some "goal oriented" numerical schemes. These numerical schemes are derived using a variety Galerkin methods such as Standard Galerkin, Semi-Streamline Diffusion, Characteristic Galerkin and Characteristic Streamline Diffusion methods. Our focus has been in two of these approx-

imation schemes: (i) the Semi-Streamline Diffusion and (ii) the Characteristic Streamline Diffusion methods.

For these two setting, we derived a priori error estimates and formulated the adaptive algorithm. Since in our numerical tests we have used a closed form of the analytic solution, therefore it suffices to use a priori error estimates for the local mesh refinements. Numerically we tested our adaptive algorithm for different type of initial data in (4.1) in three tests with different mesh refinement parameter $\widetilde{\gamma}$ in the mesh refinement criterion (5.1). The goal of our numerical experiments was to remove oscillatory behavior of the computational solution as well as removing of the formation of the artificial layer.

Using Tables and Figures of section 6 we can conclude that the oscillatory behavior of the computed solutions which were obtained in [3] are appearing for problems with non-smooth initial data and on non-refined meshes. In this work we removed these oscillations by adaptive mesh refinement and decreasing the dominance of the coefficient in the convection term.

Acknowledgments

The research of first and second authors is supported by the Swedish Research Council (VR).

References

[1] A. R. Adams, *Sobolev spaces*, Academic press, New York, 1975.

[2] M. Asadzadeh, Streamline diffusion methods for Fermi and Fokker-Planck equations, *Transport Theory Statistica Physics*, 26(3), pp. 319–340, 1997.

[3] M. Asadzadeh and E. Larsen, Linear transport equations in flatland with small angular diffusion and their finite element approximation, *Mathematical and Computer Modelling, Elsevier*, pp. 495 – 514, 2007.

[4] M. Asadzadeh, A posteriori error estimates for the Fokker-Planck and Fermi pencil beam equations, *Math. Models Meth. Appl Sci.*, V. 48, 10 (5), pp. 737–769, 2000.

[5] M. Asadzadeh and A. Sopasakis, On fully discrete schemes for the Fermi pencil-beam equation, *Comput. Methods Appl. Mech. Engrg.* 191 (1), pp. 4641–4659, 2002.

[6] M. Asadzadeh, On the stability of characteristic schemes for the fermi equation, *Appl. Comput. Math.*, 1(1), pp.158–174, 2002.

[7] C. Borgers and E. W. Larsen, Asymptotic derivation of the fermi pencil-beam approximation, *Nucl. Sci. Engrg*, 123, pp. 343–357, 1996.

[8] S. C. Brenner, L. R. Scott, *The Mathematical theory of finite element methods*, Springer-Verlag, Berlin, 1994.

[9] P. G. Ciarlet, *The finite element method for elliptic problems*, North-Holland, Amsterdam, New York, Oxford, 1980. 1941.

[10] L. Eyges, Multiple scattering with energy loss, *Phys. Rev.*, 74, pp.1534–35, 1948.

[11] C. Johnson, A new approach to algorithms for convection problems which are based on exact transport + projection, *Comput. Methods Appl. Mech. Engrg.*, 100, pp. 45–62, 1992.

[12] E. W. Larsen, C. D. Levermore, G. C. Pomraning, J. G. Sanderson, Discretization methods for one-dimensional Fokker-Planck operators. *J. Comput. Phys.* 61, no. 3, pp. 359–390, 1985.

[13] Z.-M. Luo, A. Brahme, "An Overview of the Transport Theory of Charged Particles", *Raiat. Phys. Chem.,* **41***, 673*, (1993).

[14] G. C. Pomraning, The Fokker-Planck Operator as an Asymptotic Limit, *Math. Models Meth., Ap. Sci.,* **2***, 21* (1992).

[15] A. K. Prinja, G. C. Pomraning, One-dimensional beam transport. *Transport Theory Statist. Phys.* 25, no. 2, 231–247, 1996.

[16] B. Rossi, K. Greisen, Cosmic-ray theory, *Rev. Mod. Phys.*, 13, , pp. 309–340,